

## **Spatial variability of chlorophyll and NDVI obtained by different sensors in an experimental coffee field**

S.A.S. Silva<sup>1</sup>, G.A.S. Ferraz<sup>1,\*</sup>, V.C. Figueiredo<sup>2</sup>, M.M.L. Volpato<sup>2</sup>,  
M.L. Machado<sup>2</sup>, V.A. Silva<sup>2</sup>, C.S.M. Matos<sup>2</sup>, L. Conti<sup>3</sup> and G. Bambi<sup>3</sup>

<sup>1</sup>Federal University of Lavras, School of Engineering, Department of Agricultural Engineering, Rotary Clover Professor Edmir Sá Santos, BR37200-900 Lavras, Brazil

<sup>2</sup>Agricultural Research Company of Minas Gerais, Av. José Cândido da Silveira 1647, Bairro União Belo Horizonte, BR31170-495 Belo Horizonte, Brazil

<sup>3</sup>University of Florence – UniFI, Department of Agriculture, Food, Environment and Forestry (DAGRI), Via San Bonaventura, 13, IT50145 Florence, Italy

\* Correspondence: gabriel.ferraz@ufla.br

Received: January 31<sup>st</sup>, 2024; Accepted: May 1<sup>st</sup>, 2024; Published: May 8<sup>th</sup>, 2024

**Abstract.** The objective of this research was to study the spatial variability of NDVI and chlorophyll sampled by different sensors, as well as to evaluate the correlation between them in a coffee field. The study was carried out on a coffee farm located in the municipality of Três Pontas, Minas Gerais. A sampling grid containing 30 points was created for the study area. Each sampling point was represented by one plant, which was georeferenced by a GNSS RTK. For each sample plant, NDVI and chlorophyll were obtained by the optical and active sensors GreenSeeker and ClorofiLOG, respectively. In addition, it was carried out a flight with an RPA equipped with a passive and multispectral sensor. Using the data obtained by active sensors, a geostatistical analysis was carried out to evaluate the spatial variability of NDVI and chlorophyll. The geostatistical analysis verified the existence of spatial dependence for the two attributes, and thus it was possible to generate spatialization maps through kriging. The images obtained by the passive sensor resulted in five multispectral orthomosaics, making it possible to calculate the NDVI, thus generating a spatialization map of this index. It was possible to observe in the generated maps, points that presented a certain similarity and for this purpose a correlation analysis was carried out for the values of each attribute, sampled directly in the maps, and in different sampling grids (30, 60, 90 and 120 points). By analyzing the Pearson coefficient (R) it was possible to quantify the level of correlation between the data obtained by the different sensors and through the t test it was possible to find significant correlations between them.

**Key words:** geostatistics, spatial distribution, spectral indices, active sensor, passive sensor.

### **INTRODUCTION**

The term Precision Coffee Farming (PC) originated from the application of Precision Agriculture (PA) techniques and technologies to coffee cultivation (Alves et al., 2006). It is characterized as a set of techniques, technologies, and tools that efficiently characterize the spatial variability of coffee tree parameters (Ferraz et al.,

2012; Santana et al., 2022). Through this set of characteristics, it is possible to obtain an integrated base of information and to understand the relationships between the production system, the attributes involving soil and plants, and their behavior in variations in space, time, and climate.

In PA, a very important technological tool is remote sensing (RS), widely disseminated due to its various applications. Precision agriculture combined with computational tools has been studied and widely disseminated in terms of coffee crops (Santos et al., 2023). According to Amaral et al. (2020), sensors and applications in remote sensing (RS) at all levels (orbital, aerial and terrestrial) have significantly evolved.

Spectral remote sensing enables early, efficient, objective and non-destructive assessment of plant responses to environmental stress factors (Li et al., 2010). According to Shiratsuchi et al. (2014) the sensors used by RS can be divided into two categories: passive or active. Passive sensors record electromagnetic energy reflected or emitted by the target, such as reflected solar radiation or emitted thermal radiation. Active sensors provide their own source of electromagnetic energy, such as radars, sonars, active canopy sensors (such as GreenSeeker and ClorofiLOG, for example).

The combination of spectral data from two or more bands creates vegetation spectral indices. These improve the relationship between spectral data and the biophysical parameters of vegetation (Zanzarini et al., 2013). Vegetation indices allow determining the health status of crops, based on different characteristics (Main et al., 2011; Yu et al., 2014). The normalized difference vegetation index (NDVI) is one of the technologies widely used in the field of remote sensing and has a strong relationship with morphophysiological variables, such as leaf health, leaf area index (LAI), biomass, plant productivity and chlorophyll concentration (Kim et al., 2022).

In recent years, RS methodologies have been widely used in monitoring agricultural crops and in decision-making for better management practices (Marin et al., 2019). Jesus et al. (2014) states that RS techniques have been widely used to evaluate vegetation indices and chlorophyll levels, with the aim of identifying, in real time, possible changes due to variations that may occur in cultivation. Barbosa et al. (2019) and Santos et al. (2019a) stated that the use of Remotely Piloted Aircraft (RPA) in PA has increasing potential for agricultural monitoring through obtaining data with RS techniques. RPA's can be used in smaller areas or in specific locations to obtain data in less time, being able to monitor crop growth.

By identifying the spatial variability of the vegetative development of plants, it is possible to observe differences in productive potential in coffee plantations, where in most rural properties, they are treated in a uniform manner in terms of management (Rodrigues et al., 2019). Campos et al. (2022) state that adequate management of coffee plantations can be carried out in order to make the plants well-nourished and productive through geospatial and temporal monitoring of coffee trees.

The chlorophyll content of leaves is an indicator that represents the growth status of crops, and its monitoring in crops is crucial for agricultural practices (Pereira et al., 2019). Chlorophyll can be subdivided into two classes: chlorophyll a and chlorophyll b, together with carotenoids, are part of the primary photosynthetic pigments of plants (Moreira, 2011). These photosynthetic pigments have an important role in plant physiology, as they are correlated with attributes such as nitrogen and magnesium (Marenco & Lopes, 2007) that are related to plant nutrition. Furthermore, chlorophyll absorbs energy at different wavelengths (Moreira, 2011), which makes it possible to use

remote sensing (RS) techniques to observe the behavior of this attribute in different crops (Santos et al., 2019b).

Therefore, this work aims to study the spatial variability of the normalized difference vegetation index and chlorophyll obtained by active and passive sensors, as well as to evaluate the correlation between the data obtained by them in different sampling grids in coffee fields.

## MATERIALS AND METHODS

The study was carried out in a coffee plantation located in an Experimental Field belonging to the Agricultural Research Company of Minas Gerais (EPAMIG, acronym in portuguese), located in the municipality of Três Pontas, southern region of the state of Minas Gerais, Brazil, at mean altitude of 905 m above sea level in the coordinates of the Universal Transverse Mercator (UTM) system S 7640030.4 and E 449531.5, Zone 23K. This municipality has at mean annual temperature of 20.3 °C and a mean annual precipitation of 1,429 mm. The soil in this area is classified as Oxisol.

The experimental area comprised 1.2 ha of coffee trees of the *Coffea arabica* L. species, cultivar Topázio MG 1190. This crop was established in 1998 with spacing between rows of 3.70 m and 0.70 m between plants (Fig. 1).

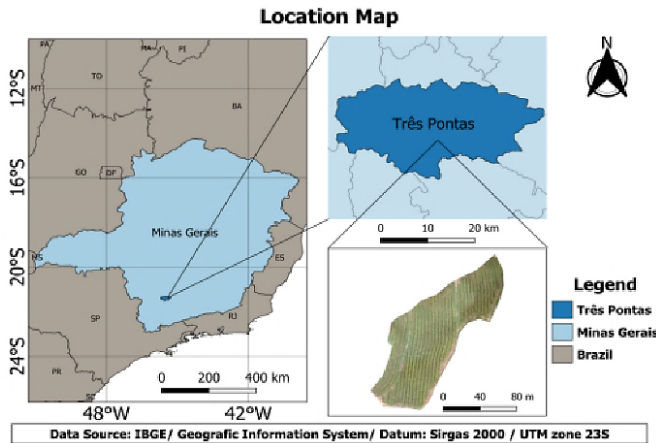


**Figure 1.** Location map.

In this area, a sampling grid was developed containing 30 georeferenced points (Fig. 2), where sample data for the variables  $NDVI_{ps}$  (NDVI obtained from RPA images),  $NDVI_{as}$ ,  $NDVI_{as.east}$  and  $NDVI_{as.west}$  (NDVI obtained by GreenSeeker readings) and Chlorophyll. Each sampling point was represented by a plant. Both the study area and sampling points were georeferenced by a global navigation satellite system (GNSS) real-time kinematic (RTK).

The data collection for this study was conducted in August 2022. All measurements with the different sensors were carried out simultaneously in the interval from 11:00 am to 12:00 pm. The methodology involved several steps, including field data collection, data processing, generation of maps, and comparison of values.

## Field data collection

### Chlorophyll

Chlorophyll data were acquired employing an active sensor, designated as chlorofiLOG, produced by Falker. The measurement by this sensor is conducted optically, utilizing the optimal light frequencies absorbed by chlorophyll during photosynthesis. This instrument assesses three frequency bands and can discriminate between the two chlorophyll types: Chlorophyll a and Chlorophyll b. Each sampled plant was stratified into three sections (upper, middle, and lower), and the chlorophyll measurements was specifically taken from the middle section. Ten leaves were selected from either the third or fourth node from the apex of the plagiotropic branch, ensuring they were healthy and devoid of signs of pests or diseases (Santos et al., 2022; Bento et al., 2022; Barata et al., 2023). Sampling occurred around 11:00 a.m., coinciding with the timing of the Remote Piloted Aircraft (RPA) flight for image collection. In total, 300 chlorophyll readings were recorded, resulting in a dataset comprising 30 attribute values, derived from the mean of 10 readings per sampled plant.

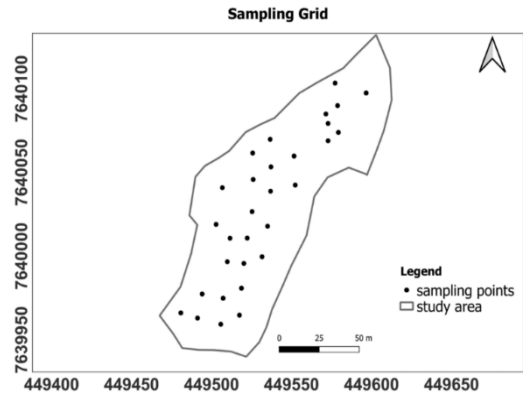


Figure 2. Sample grid.

### NDVI active sensor (NDVI<sub>as</sub>)

For the Normalized Difference Index (NDVI) readings obtained by an active sensor (NDVI<sub>as</sub>), the commercial GreenSeeker® 505 HandHeld Sensor was used, which is a non-image-forming optical sensor capable of measuring this index. The measurements of this index using this device were carried out using a method similar to scanning.



Figure 3. NDVI data sampling using the active sensor.

For NDVI<sub>as</sub> data sampling, the plant was divided into three sections, referred to as thirds (upper, middle, and lower), and two sides of solar exposure (east and west) were considered. On each side of sun exposure, 9 readings were taken, with 3 in each third. represented by Fig. 3. So, 540 NDVI<sub>as</sub> values were obtained, divided into 18 readings

for each sample plant (considering the 9 readings obtained for the east side and the 9 readings obtained for the west side). The readings were divided as follows:  $NDVI_{as}$  (mean of 18 readings obtained in the three thirds of the plants for the east and west sides),  $NDVI_{as,east}$  (mean of 3 readings obtained from the upper third of the sample plants facing east) and  $NDVI_{as,west}$  (mean of 3 readings obtained in the upper third of the sample plants facing west).

This methodology for NDVI readings obtained by the GreenSeeker sensor was adopted considering that due to the high height of the coffee trees (above 2 m) it would be impossible to read the crown of the plants.

### **NDVI passive sensor ( $NDVI_{ps}$ )**

To generate NDVI values by the passive sensor ( $NDVI_{ps}$ ), a flight was carried out with an RPA, model EBee SQ from the manufacturer senseFly. This aircraft has the following characteristics: fixed wing, a wingspan of 110 cm, rated radio range of 3 km, cruising speed of 40–110 km h<sup>-1</sup>, wind resistance of up to 45 km h<sup>-1</sup> (12 m s<sup>-1</sup>), electric motor, maximum payload of 1.1 kg (including camera and batteries) and flight autonomy of up to 55 min.

The aircraft was equipped with a Parrot camera (Sequoia model) with a high-resolution red-green-blue (RGB) sensor with a focal length of 4.88 mm. This camera also has four monochromatic sensors for the spectral bands: green (550 ± 40 nm), red (660 ± 40 nm), near infrared (NIR) (790 nm ± 40 nm) and red edge (735 ± 40 nm). The resolution is 1,280×960, with a pixel size of 3.75 µm and a focal length of 3.98 mm; the ground sample distance (GSD) is 6.8 cm at a flight height of 50 m (above ground level – AGL), which was adopted for the described study.

In addition to the RGB and monochromatic sensors, Sequoia has a luminosity sensor to correct the influence of the sun by obtaining data with radiometric corrections. This sensor records not only the current lighting, but also the location of the center of the the photo and inertial data.

Flight planning and execution was carried out through the base station, which was developed by the same aircraft manufacturer (senseFly) with the following set: the eMotion software, responsible for flight programming and execution of the aircraft's path, and a transmitting antenna that allows real-time monitoring of the overflight, as well as sending commands for landing,

direction changes and image acquisition. During the flight, images are stored on the memory card contained in the multispectral sensor. After the flight, these images will be downloaded and sent to processing software. The flight plan followed the parameters represented in Table 1.

**Table 1.** Flight planning parameters

Camera	Parrot Sequoia
Resolution of the RGB camera	16 megapixels
Resolution of the multispectral camera	1.2 megapixels
Focal length	3.98mm
Vertical cover	70%
Horizontal cover	70%
Spatial resolution	6.8 cm
Flight altitude	50 m
Speed	12 m s <sup>-1</sup>

### **Processing of data obtained by active Chlorophyll and $NDVI_{as}$ sensors**

Chlorophyll measurements using the ClorofiLOG sensor were downloaded using specific software provided by the equipment manufacturer. In this way, it was possible

to download the measurements stored in the device and determine chlorophyll a (Chla) and chlorophyll b ( Chlb). The sum of these two types of chlorophyll (Chla + Chlb) results in Total Chlorophyll (TC), which was used in this work.

Mean values of NDVI<sub>as</sub>, NDVI<sub>as.east</sub>, NDVI<sub>as.west</sub>, and chlorophyll were utilized to analyse the spatial dependence of these attributes using semivariograms. Semivariance is classically estimated by Eq. (1), according to Vieira (2000).

$$\hat{\gamma}(h) = \frac{1}{2 N(h)} \sum_{i=1}^{Ni=(h)} [Z(x_i) - Z(x_i + h)]^2 \quad (1)$$

Where N(h) is the number of experimental pairs of observations Z(xi) and Z(xi + h), separated by a distance h. The semivariogram is represented by the graph  $\hat{\gamma}(h)$  versus h. From the adjustment of a mathematical model to the calculated values of  $\hat{\gamma}(h)$ , the coefficients of the theoretical model are estimated for the semivariogram, called nugget effect (C<sub>0</sub>), contribution (C<sub>0</sub> + C<sub>1</sub>) and range (a), as described by Bachmaier & Backers (2008).

For this study, the ordinary least squares (OLS) method and spherical model were used to fit the semivariogram. To check whether the model adjustments met the cross-validation requirements, the mean error (ME) was calculated according to Isaaks & Srivastava (1989). The ME must have a value as close to zero as possible.

After adjusting the semivariograms and verifying spatial variability, the data were interpolated using ordinary kriging. Thus, the variables were estimated in locations where they were not sampled, which made it possible to visualize their distribution in space through thematic maps.

The calculation of the degree of the spatial dependence (DSD) of the variables followed the classification proposed by Cambardella et al. (1994). In this classification, the authors point out that there is strong spatial dependence when the semivariogram presents a nugget effect equal to or less than 25% of the sill variance, moderate spatial dependence when this relationship is between 25% and 75%, and weak spatial dependence when it is greater than 75%.

The geostatistical analysis carried out by adjusting the semivariograms and ordinary kriging was carried out in the RStudio software using the geoR package (Ribeiro Jr & Diggle, 2001). Kriging generated interpolated and georeferenced points, which were exported to the QGIS version 3.22.9 software to create isocolour maps for the attributes NDVI<sub>as</sub>, NDVI<sub>as.east</sub>, NDVI<sub>as.west</sub> and chlorophyll.

### **Processing of NDVI data obtained by the passive sensor**

The normalized difference index (NDVI) consists of calculating the difference between emission and reflection of two wavelengths of the electromagnetic spectrum: near infrared (0.725–1.1 μm) and red (0.58–0.68 μm) (Rouse et al., 1973).

After completing the flight and capturing images using the multispectral camera, the images were processed using the Pix4D software, resulting in four orthomosaics for the spectral bands and one orthomosaic for the RGB composition. The orthomosaics were imported to the geoprocessing software QGIS, where NDVI was calculated using the raster calculator tool and using Eq. 2, enabling to obtain the NDVI values for the study area.

$$NDVI = \frac{NIR - RED}{NIR + RED} \quad (2)$$

where NIR – near infrared spectral band; RED – red spectral band

The NDVI value varies from -1 to 1 and shows us the vigor of the crop. Values close to 1 mean that the more intense the green, the more vigor there is in the vegetation and vegetation cover. We must take into account whether we are working with extensive or intensive cultivation, or if there is no bare soil, as all of this will be taken into account by the index. And this will also measure the vigor of the weeds. Values close to 0 correspond to areas with little vegetation, initial stages of cultivation, bare soil or non-productive areas. Negative values are generally associated with areas of water, snow, or clouds.

### **Map generation and correlation analysis**

For this study, five maps were generated, one map through the calculation of NDVI using multispectral images (NDVI<sub>ps</sub>) and four maps obtained by geostatistical analysis through ordinary kriging (NDVI<sub>as</sub>, NDVI<sub>as.east</sub>, NDVI<sub>as.west</sub>, and chlorophyll). All maps were created using QGIS software. To compare map values of the studied variables, 4 sample grids of 30, 60, 90 and 120 points were created within the area. To construct the grids, the following requirements were used:

- Points have a minimum distance of 2 m from each other;
- The points are 4 m away from the area's borders, so that there would be no interference in the results.

Polygons of 0.8 m were created using the zonal statistical tool for each sampling point within the grids. These polygons were then sampled using the mean pixel values within the 0.8 m buffer for each sample point across the different grids.

The sampling of NDVI data, for both sensors, and chlorophyll values resulted in 4 tables, each of which is represented by a sampling grid. With the data from the tables, it was possible to perform correlation analysis using the RStudio software through the ggplot2 library. Correlation analysis summarizes the degree of relationship of two or more variables, its calculation results in the Pearson Correlation Coefficient (R). For its validation, the test followed the criteria:

$\rho \leq 0.05$ : significant at the 5% probability level

$\rho > 0.05$ : not significant.

## **RESULTS AND DISCUSSION**

### **Descriptive statistics**

Table 2 presents the data from the descriptive statistical analysis of the variables under study that were obtained by the sensors directly and indirectly in the field. In the table it is possible to observe the minimum, maximum, median, mean, variance, standard deviation and coefficient of variation values for the attributes: NDVI<sub>as</sub>, NDVI<sub>as.east</sub>, NDVI<sub>as.west</sub> and chlorophyll.

**Table 2.** Descriptive statistics of data

Attribute	Minimum	Maximum	Median	Mean	Variance	SD	CV (%)
NDVI <sub>ps</sub>	0.27	0.77	0.51	0.51	0.01	0.13	25.87
NDVI <sub>as</sub>	0.80	0.89	0.86	0.86	3.73	0.01	2.28
NDVI <sub>as.east</sub>	0.40	0.79	0.65	0.64	0.01	0.09	15.56
NDVI <sub>as.west</sub>	0.43	0.75	0.64	0.62	0.01	0.10	16.14
Chlorophyll	40.10	64.20	52.44	52.44	29.71	5.45	10.39

SD: standard deviation; CV: coefficient of variation.

From descriptive statistics it is possible to observe that the mean for NDVI values was higher when considering all thirds and the east and west faces for GreenSeeker readings (mean NDVI<sub>as</sub> = 0.86), while the means for NDVI<sub>ps</sub>, NDVI<sub>as.east</sub> and NDVI<sub>as.west</sub> were very close (0,51, 0.64,0.62) respectively. Regarding chlorophyll, the mean for this attribute was 52.44.

Gomes & Garcia (2002) state that the variability of an attribute can be classified according to the magnitude of its coefficient of variation (CV), which according to the authors can be: low, when this is less than 10%; moderate when it is in the range of 10 to 20%, high when it is between 20 and 30%; and very high when it is above 30%. Frogbrook et al. (2002) state that the first indicators of data heterogeneity are high CV values. According to the CV values represented in Table 2, we can state that the attribute NDVI<sub>ps</sub> represent high variability, while the attributes NDVI<sub>as.east</sub>, NDVI<sub>as.west</sub> and chlorophyll represent moderate variability in their data sets, the NDVI<sub>as</sub> presented low variability (2.28%).

### Geostatistical analysis

Table 3. shows the semivariogram adjustment parameters, as well as the mean error values and degree of spatial dependence.

**Table 3.** Semivariogram adjustment parameters for the variables under study

variable	C <sub>0</sub>	C <sub>1</sub>	C <sub>0</sub> +C <sub>1</sub>	a	DSD (%)		ME
NDVI <sub>as</sub>	0.01	3.50	3.51	40	0.28	Strong	0.0000
NDVI <sub>as.east</sub>	0.00	0.01	0.01	45	0.00	Strong	0.0001
NDVI <sub>as.west</sub>	0.00	0.01	0.01	25	0.00	Strong	0.0009
Chlorophyll	0.01	20.00	20.01	65	0.05	Strong	0.0031

C<sub>0</sub>: nugget effect; C<sub>1</sub>: sill; C<sub>0</sub>+C<sub>1</sub>: contribution; a: range; DSD: degree of the spatial dependence and ME: mean error.

Through the results of the geostatistical analysis, it was observed that, for all variables, the ME presented very low values and close to zero, demonstrating that the adjustments made by the spherical model were well made and met the cross-validation requirements. All variables represented ME values very close to zero.

This study identified that all variables studied showed a strong degree of spatial dependence (DSD).

### Thematic maps

Fig. 4 represents the maps of NDVI (Passive sensor), NDVI (Active sensor), NDVI (Active sensor - East), NDVI (Active sensor - West), and Chlorophyll respectively.

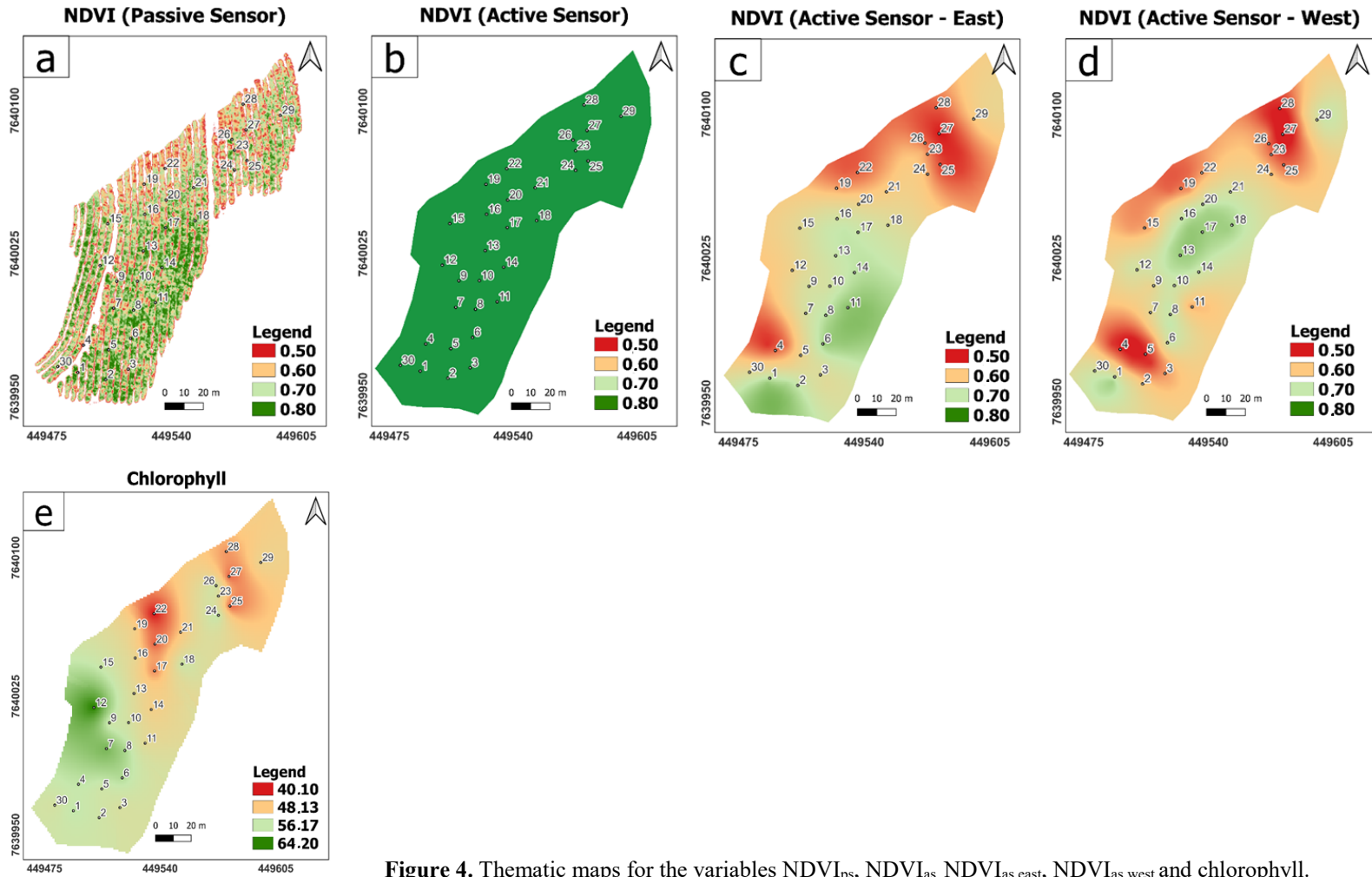


**Figure 4.** Thematic maps for the variables  $NDVI_{ps}$ ,  $NDVI_{as}$ ,  $NDVI_{as.east}$ ,  $NDVI_{as.west}$  and chlorophyll.

The maps represented by Fig. 4 were created in the same color palette and also in the same range of values for the NDVI attribute (Figs 4, a; 4, b; 4, c and 4, d).

When analyzing Table 2, it is possible to observe that the NDVI index obtained by the passive sensor varied from the lowest value of 0.27 to the highest value of 0.77, however, during the construction of the thematic map, it was observed that NDVI values below 0.50 were related to exposed soil, low vegetation and drought between the rows of coffee trees, so to facilitate the visualization of only the NDVI values in the coffee plants, NDVI values below 0.50 were omitted in the image, facilitating the comparison between the values of NDVI obtained actively by the interpolated maps.

The visual analyzes that will be presented below will disregard Fig. 4, b, due to the little variation in its values (0.80 to 0.89 Table 2) the thematic map was represented by only one tone (dark green) which makes discussion difficult. of this image with the results obtained by the other methods in images 4, a, 4, c, 4, d and 4, e.

When looking at Fig. 4, a, it is possible to state that most of the coffee trees had NDVI values in the range of 0.60 to 0.70. It is also possible to state that when drawing an imaginary line dividing the area into two hemispheres, the north of the area (above point 16) presents lower NDVI values, unlike the south side of the area (below point 16) where it is possible to find some concentrations of higher values (NDVI around 0.80). Throughout the area it is possible to observe some points with low NDVI values (around 0.50) mainly in the coffee trees close to points 19 and 22 and also close to points 23, 26, 27 and 28, which is also observed in the Figs 4, c and 4, d.

In relation to Figs 4, c and 4, d, it is possible to observe that the NDVI values coincide in a large part of the area. A small difference is observed between the NDVI values only in coffee trees close to sampling points 3.5, 11, 15, 29 and in the zone below points 1.2 and 30. Furthermore, it is possible to observe that to the north of the area in Figs 4, c and 4d the NDVI values are lower when compared to the values in the southern part of the area, this same situation is found in Fig. 4, a. This can be justified due to the northern part of the area, mainly around points 19, 22, 23, 25, 26, 27 and 28, which are next to a very busy rural road that accesses a coffee processing plant, therefore, Coffee trees closer to both the road and the plant are affected by dust as well as higher temperatures, generating a greater set of stress on the coffee plants.

When analyzing the map represented by Fig. 4, e, it is observed that lower chlorophyll values (around 40.10) are concentrated around points 19 and 22 and also close to points 23, 25, 27 and 28, coinciding with the lower NDVI values of Figs 4, a, 4, c and 4, d. Regarding the highest chlorophyll values, these are found in coffee trees close to point 12 (southwest of the area), values that coincide with the NDVI values found in Fig. 4, a.

Visual analysis of the maps is the first step to identify the existence of a possible correlation between the variables and the methods used, however a mathematical analysis is necessary to quantify the relationship between them, as well as verify their significance. Therefore, a correlation analysis was carried out by calculating the **Pearson** coefficient (R) as well as performing the t test to determine significance.

### **Correlation analysis**

In the literature, there are studies that evaluate the correlation between  $NDVI_{ps}$  x Total Chlorophyll (Bento et al., 2022; Santos et al., 2022 and Barata et al., 2023) as well as researches that evaluate the correlation of NDVI obtained by actives and passive

sensors (Gomes et al., 2021 and Campos et al., 2022) in coffee cultivation. This research will be important to provide a basis for discussing the results presented in this paper.

In Fig. 5 it is possible to observe the correlation graphs for the variables  $NDVI_{ps}$ ,  $NDVI_{as}$ ,  $NDVI_{as.east}$ ,  $NDVI_{as.west}$ , and chlorophyll. Table 4 shows the  $\rho$  values for each variable and sampling grid used in this study in order to verify their significance using the t test.

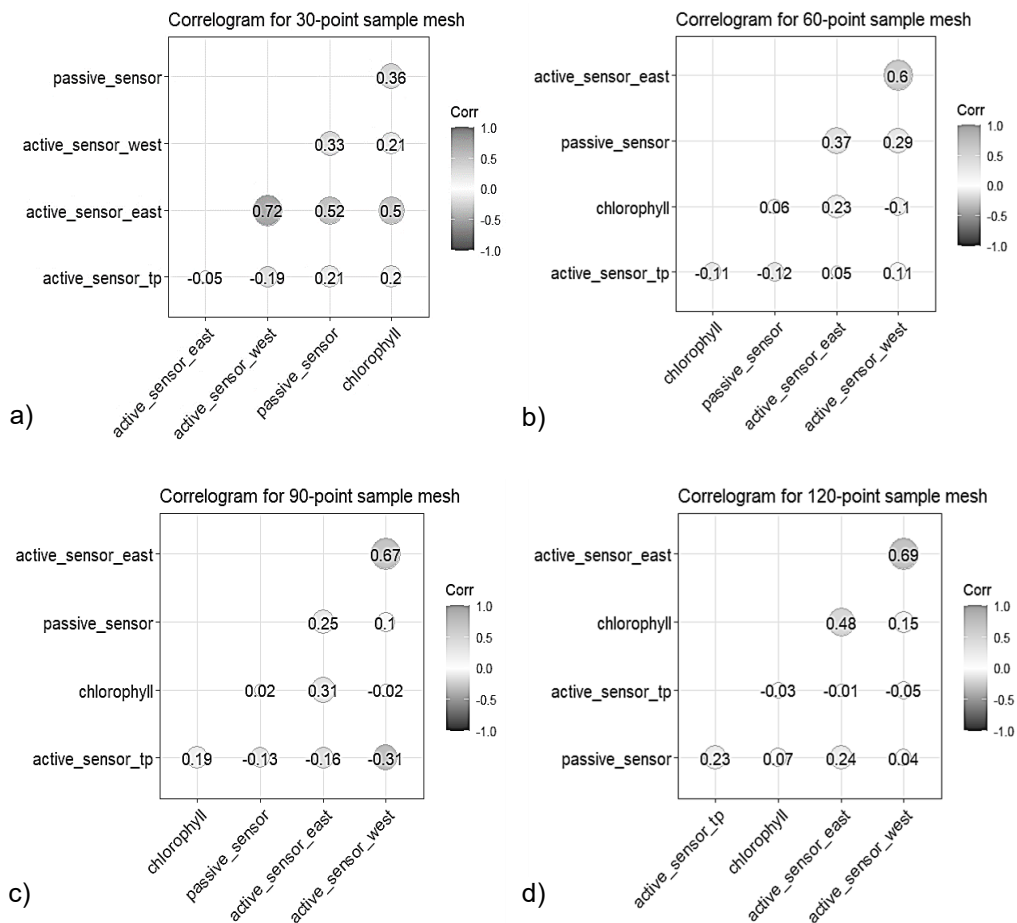


**Figure 5.** Correlograms for sample grides with 30 points (a), 60 points (b), 90 points (c) and 120 points (d).

Considering the data presented by the correlogram in Fig. 5, a, as well as the  $\rho$  values present in Table 4, it can be stated that the results of the 30-point sampling grid indicate that the  $NDVI_{as.east} \times NDVI_{ps}$  presented a correlation of 52%,  $NDVI_{as.east} \times NDVI_{as.west}$  of 72% and  $NDVI_{as.east} \times Chlorophyll$  of 50%.

In relation to the 60-point sampling grid, it can be observed that there was a significant correlation between  $NDVI_{ps} \times NDVI_{as.east}$  and  $NDVI_{ps} \times NDVI_{as.west}$ , with correlations of 37% and 29% respectively. Also, for this grid, a significant correlation

of 60% can be observed when comparing the NDVI values measured by GreenSeeker on the east and west faces ( $NDVI_{as.east}$  and  $NDVI_{as.west}$ ).

**Table 4.**  $\rho$  value for correlations between variables in different sampling grids

Grid	Variable	$NDVI_{ps}$	$NDVI_{as}$	$NDVI_{as.east}$	$NDVI_{as.west}$	Chl
30	$NDVI_{ps}$	0.00	0.27ns	0.00 **	0.07ns	0.05ns
	$NDVI_{as}$	0.26ns	0.00 ns	0.78ns	0.32ns	0.30ns
	$NDVI_{as.east}$	0.00ns	0.78ns	0.00	0.00 **	0.00 **
	$NDVI_{as.west}$	0.07ns	0.32ns	0.00 **	0.00	0.27ns
	Chl	0.05ns	0.30ns	0.00 **	0.27ns	0.00 ns
60	$NDVI_{ps}$	0.00	0.37ns	0.00 **	0.02 **	0.66ns
	$NDVI_{as}$	0.37ns	0.00	0.07ns	0.38ns	0.42ns
	$NDVI_{as.east}$	0.00 **	0.73ns	0.00	0.00 **	0.08ns
	$NDVI_{as.west}$	0.02 **	0.38ns	0.00 **	0.00	0.44ns
	Chl	0.66ns	0.42ns	0.08ns	0.44ns	0.00
90	$NDVI_{ps}$	0.00	0.23ns	0.01 **	0.35ns	0.81ns
	$NDVI_{as}$	0.23ns	0.00	0.13ns	0.00 **	0.08ns
	$NDVI_{as.east}$	0.02 **	0.13ns	0.00	0.00 **	0.00 **
	$NDVI_{as.west}$	0.35ns	0.00 **	0.00 **	0.00	0.87ns
	Chl	0.81ns	0.08ns	0.00 **	0.86ns	0.00
120	$NDVI_{ps}$	0.00	0.01 **	0.00 **	0.62ns	0.46ns
	$NDVI_{as}$	0.01 **	0.00	0.90ns	0.55ns	0.71ns
	$NDVI_{as.east}$	0.00 **	0.90ns	0.00	0.00 **	0.00 **
	$NDVI_{as.west}$	0.62ns	0.55ns	0.00 **	0.00	0.09ns
	Chl	0.47ns	0.71ns	0.00 **	0.09ns	0.00

\*\* : significant at the 5% level; ns : not significant.

When considering the sampling grid of 90 points, a significant correlation can be observed between  $NDVI_{ps}$  x  $NDVI_{as.east}$  (25%) and a significant and inverse correlation of -31% when comparing  $NDVI_{as}$  and  $NDVI_{as.west}$ . The  $NDVI_{as.east}$  variable, In addition to its correlation with  $NDVI_{ps}$ , this variable also showed correlations of 67% and 31% with the  $NDVI_{as.west}$  and Chlorophyll variables.

For the 120-point sampling grid, significant correlations can be observed between  $NDVI_{ps}$  x  $NDVI_{as}$  (23%) and  $NDVI_{ps}$  x  $NDVI_{as.east}$  (24%), as well as between  $NDVI_{as.east}$  x  $NDVI_{as.west}$  (69%) and  $NDVI_{as.east}$  x Chlorophyll (48%).

A general comparison of the variables that were correlated, it was observed that the variable that presented the highest number of correlations was the  $NDVI_{as.east}$  (11 correlations) and it was also possible to observe that for the grides of 60, 90 and 120 points this variable presented a correlation significant with  $NDVI_{ps}$ . The variable that presented the lowest number of correlations was  $NDVI_{as}$  (only 2 significant correlations), this was already reflected in the discussion topic of the maps, where it was possible to observe the little variation in values of this variable. Regarding Chlorophyll, it presented only 3 significant correlations, and all cases were significantly correlated with the  $NDVI_{as.east}$  for the 30, 90 and 120 point grids.

Another noteworthy observation is the comparison between the  $NDVI_{as.east}$  and  $NDVI_{as.west}$  variables across all sample grids. A significant correlation was observed between these variables; however, despite their statistical significance, they exhibited moderate correlations (72% for the 30-point grid, 60% for the 60-point grid, 67% for the

90-point grid and 69% for the 120-point grid). This indicates that despite utilizing the same data collection method with the GreenSeeker and considering only the readings from the upper third of the plant, these variables did not display high correlations. This observation can be attributed to the environmental conditions during data collection. Specifically, the shaded west side resulted in lower NDVI values, while the east-facing side of the plants, illuminated by sunlight, generated higher NDVI values. Additionally, there were more correlations observed with the NDVI<sub>ps</sub> variable, as the RPA image collection coincided with peak solar irradiance and absence of cloud cover.

Santos et al. (2022) investigated the effectiveness of various vegetation indices derived from multispectral imagery captured by a remotely piloted aircraft (RPA)-mounted sensor in predicting chlorophyll content in both coffee tree leaves (Chl<sub>leaf</sub>) and canopy (Chl<sub>dossel</sub>). They also examined the correlation between these indices and chlorophyll levels across different seasons (rainy and dry). The study reported a significant correlation of 61% between NDVI<sub>ps</sub> and Total Chlorophyll during the dry season (the same season and chlorophyll content used in our study). However, our research did not observe a significant correlation between these same attributes. By collecting data such as height, diameter, and chlorophyll, and together with high-resolution multispectral images obtained by RPA, Bento et al. (2022) evaluated the relationship between vegetation indices with total chlorophyll (TC) content and leaf area index to characterize different types of coffee cultivars. To evaluate the correlation between these attributes and vegetation indices, the authors used the Spearman correlation index. Through correlation between the NDVI<sub>ps</sub> and TC, the authors found inverse and non-significant correlations of -0.05, -0.15 and -0.18 for the cultivars Catucaí 2SL, Catucaí IAC62 and Bourbon IACJ10 respectively, corroborating the results of this study. work, despite the difference between age and cultivars of coffee trees.

Barata et al. (2023), evaluating coffee trees transplanted to areas with different liming methods (surface and deep) through field measurements and vegetation indices obtained by RPA images, carried out a correlation analysis between VI and parameters such as height, crown diameter, chlorophyll, leaf area index, chlorophyll a, chlorophyll b and total chlorophyll. The results obtained by the authors for the correlation between NDVI<sub>ps</sub> and Total Chlorophyll do not show significant correlations and once again corroborate the results found in this research.

Gomes et al. (2021) compared the NDVI obtained by active (GreenSeeker) and passive sensors (Mica Sense and MAPIR). These authors found high and significant correlations (around 80 to 90%) when comparing the NDVI<sub>ps</sub> (MicaSense multispectral sensor) in relation to the NDVI values obtained by GreenSeeker. These results differ from those found in this research, which despite significant correlations between these attributes, none presented such high values.

The discrepancy between the findings of this study and those presented by Gomes et al. (2021) lies in the methodology used by the authors to collect the index. For each sampling point, the authors carried out 3 readings using GreenSeeker, but these readings were carried out in the coffee tree canopy (at a distance of 30 cm from the plant canopy), therefore, the authors obtained values very close to those obtained by NDVI<sub>ps</sub>. In this study, it was not possible to obtain NDVI measurements using the GreenSeeker from the crown of the sample plants, since, as it was a very old coffee tree (around 25 years old), the plants were very tall (above 2 m in height, on mean), making it possible to obtain only data from the upper third.

Campos et al. (2022), evaluating the modeling of NDVI in coffee trees through the use of a passive RGB sensor coupled to RPA, evaluated the correlation of the NDVI obtained by GreenSeeker with red, blue, green bands and the normalized relationship between the RGB sensor bands. The authors find inverse and significant correlations (mean of 70% correlation between the bands evaluated). Like Gomes et al. (2021), the authors carried out NDVI readings with GreenSeeker in the coffee tree canopy, at a distance of 1m, following a methodology recommended by Ali & Ibrahim (2020).

Enciso et al. (2019), evaluating the correlation of the GreenSeeker sensor and the NDVI obtained by a multispectral sensor embedded in an RPA, observed a non-significant correlation ( $\rho < 0.05$ ), the justification is that the GreenSeeker measurements consider the plant canopy, while the NDVI calculated from multispectral images consider the entire vegetative area, resulting in an R of less than 0.45.

## CONCLUSION

The geostatistical analysis was efficient to evaluate the spatial variability of chlorophyll and NDVI data obtained by the GreenSeeker and ClorofiLOG sensors. Through geostatistical analysis it was possible to model the data and generate semivariograms and perform ordinary kriging. The data resulting from ordinary kriging generated spatial distribution maps of these two attributes, and through visual analysis it was possible to observe the behavior of these two variables throughout the study area, indicating points of highest and lowest concentration of NDVI and chlorophyll attributes.

In addition to the maps generated by kriging, the flight and processing of images obtained by RPA resulted in the calculation and generation of the NDVI<sub>ps</sub> map. Considering the very high resolution of the images, it was possible to verify with detail and precision the spatial distribution of this vegetation index in the studied area, facilitating the identification of points with higher and lower concentrations of vegetative vigor.

By calculating the Pearson correlation coefficient (R), it was possible to find significant correlations between the attributes, even when evaluated in different sampling grids. The results generated indicate the effectiveness of using sensors in coffee crops, benefiting producers in making decisions regarding the management of their crops quickly and efficiently.

**ACKNOWLEDGEMENTS.** The authors would like to thank the financial support of the funding agencies CNPQ (project 305953/2020-6), FAPEMIG (projects PPE-00118-22 and BPD-00040-22), EMBRAPA Café - Consórcio Pesquisa Café (projects 10.18.20.023.00.00 and 10.18.20.041.00.00), CAPES, and the UFLA Postgraduate Program in Agricultural Engineering.

## REFERENCES

Ali, A.M. & Ibrahim, S.M. 2020. Wheat grain yield and nitrogen uptake prediction using at Leaf and GreenSeeker portable optical sensors at jointing growth stage. *Information Processing in Agriculture* 7(3), 375–383.

- Alves, E.A., Queiroz, D.M. & Pinto, F.A.C. 2006. Precision coffee farming. In: Zambolim, L. (ed): Boas agricultural practices in coffee production, e. g. 190 (in Portuguese).
- Amaral, L.R.D., Zerbato, C., Freitas, R.G.D., Barbosa Júnior, M.R. & Simões, I.O.P.D.S. 2020. UAV applications in Agriculture 4.0. *Revista Ciência Agronômica* **51**, e20207748.
- Bachmaier, M. & Backers, M. 2008. Variogram or semivariogram? Understanding the variances in a variogram. 2008. *Precision Agriculture* **9**, 173–175.
- Barata, R.A.P., Ferraz, G.A.S., Bento, N.L., Soares, D.V., Santana, L.S., Marin, D.B., Mattos, D.G., Schwerz, F., Rossi, G., Conti, L. & Bambi, G. 2023. Evaluation of Coffee Plants Transplanted to an Area with Surface and Deep Liming Based on Multispectral Indices Acquired Using Unmanned Aerial Vehicles. *Agronomy-Basel* **13**, 2623.
- Barbosa, B.D.S., Ferraz, G.A.S., Gonçalves, L.M., Marin, D.B., Maciel, D.T., Ferraz, P.F.P. & Rossi, G. 2019. RGB vegetation indices applied to grass monitoring: A qualitative analysis. *Agronomy Research* **17**(2), 349–357.
- Bento, N.L., Ferraz, G.A.S., Barata, R.A.P., Soares, D.V., Santos, L.M. Dos., Santana, L.S., Ferraz, P.F.P., Conti, L. & Palchetti, E. 2022. Characterization of Recently Planted Coffee Cultivars from Vegetation Indices Obtained by a Remotely Piloted Aircraft System. *Sustainability* **14**, 1446. <https://doi.org/10.3390/su14031446>
- Cambardella, C.A., Moorman, T.B., Novak, J.M., Parkin, T.B., Karlen, D.L., Turco, R.F. & Konopka, A.E. 1994. Field-scale variability of soil properties in central Iowa soils. *Soil Sci. Soc. Am. J.*, **58**, 1501–1511.
- Campos, G.A. De Oliveira., Alves, M. De Carvalho., Miranda, J. Da Rocha., Resende, M.L.V. & Carvalho, G.R. 2022. Modeling coffee NDVI using passive RGB sensor embedded in UAS. *Theoretical and Applied Engineering* **6**(3), 1–11 (in Portuguese).
- Enciso, J., Avila, C.A., Jung, J., Elsayed-Farag, S., Chang, A., Yeom, J., ... & Chavez, J.C. 2019. Validation of agronomic UAV and field measurements for tomato varieties. *Computers and Electronics in Agriculture* **158**, 278–283.
- Ferraz, G.A.S., Silva, F.M.D., Carvalho, L.C., Alves, M.D.C. & Franco, B.C. 2012. Spatial and temporal variability of phosphorus, potassium and productivity of a coffee crop. *Engineering Agrícola* **32**(1), 140–150 (in Portuguese).
- Frogbrook, Z.L., Oliver, M.A., Salahi, M. & Ellis, R.H. 2002. Exploring the spatial relations between cereal yield and soil chemical properties and the implications for sampling. *Soil Use and Management* **18**(1), 1–9.
- Gomes, A., Queiroz, D.M.D., Valente, D.S., Pinto, F.D.A.D.C. & Rosas, J.T. 2021. Comparing a single-sensor camera with a multisensor camera for monitoring coffee using crop unmanned aerial vehicles. *Agricultural Engineering* **41**, 87–97.
- Gomes, F.P. & Garcia, C.H. 2002. *Statistics applied to agronomic and forestry experiments*. FEALQ, Piracicaba-Brazil, 305 pp. (in Portuguese).
- Isaaks, E.H. & Srivastava, R.M. 1989. *An introduction to applied geostatistics*. New York: Oxford University Press, Oxford, 560 pp.
- Jesus, M.H., Bredemeier, C., Vian, A.L., Almeida, D. & Silva, J.A. 2014. Variation in the vegetation index by normalized difference in corn as a function of productive potential and plant density. In: *Brazilian Congress of Precision Agriculture (ConBAP)*. São Pedro, São Paulo, BR (in Portuguese).
- Kim, K.H., Shawon, M.R.A., An, J.H., Lee, H.J., Kwon, D.J., Hwang, I.C., ... & Choi, K.Y. 2022. Effect of shade screen on sap flow, chlorophyll fluorescence, NDVI, plant growth and fruit characteristics of cultivated paprika in greenhouse. *Agriculture* **12**(9), 1405.
- Li, G., Wan, S., Zhou, J., Yang, Z. & Qin, P. 2010. Leaf chlorophyll fluorescence, hyperspectral reflectance, pigments content, malondialdehyde and proline accumulation responses of castor bean (*Ricinus communis* L.) seeds to salt stress levels. *Industrial crops and products*, **31**, 13–19.

- Main, R., Cho, M.A., Mathieu, R., O'Kennedy, M.M., Ramoelo, A. & Koch, S. 2011. An investigation into robust spectral indices for leaf chlorophyll estimation. *ISPRS* **66**(6), 751–761.
- Marengo, R.A. & Lopes, N.F. 2007. *Plant physiology: photosynthesis, respiration, water relations and mineral nutrition*. Editora UFV, Viçosa, Minas Gerais, Brazil, 469 pp. (in Portuguese).
- Marin, D.B., Alves, M.D.C., Pozza, E.A., Gandia, R.M., Cortez, M.L.J., & Mattioli, M.C. 2019. Multispectral remote sensing in the identification and mapping of biotic and abiotic variables in coffee. *Revista Ceres* **66**, 142–153 (in Portuguese).
- Moreira, M.A. 2011. *Fundamentals of Remote Sensing and Application Methodologies*. Editora UFV, Viçosa, Minas Gerais, Brazil, 422 pp. (in Portuguese).
- Pereira, A., Ribeiro, G., Oliveira, A., Oliveira, A., Ribeiro, A., Oliveira, A., Oliveira, Z. & Yang, X. 2019. Modeling aboveground biomass of maize based in machine learning approaches using remote sensing data from UAVs. *Plant Methods* **15**, 1–19.
- Ribeiro Junior, P.J. & Diggle, P.J. 2001. GeoR a package for geostatistical analysis. *R-News, New York*, **1**(2), 14–18.
- Rodrigues, G.C., Grego, C.R., Luchiari, A. & Speranza, E.A. 2019. Spatial characterization of vegetation indices relative chlorophyll index in specialty coffee production areas in southern Minas Gerais. In: *X Brazilian Coffee Research Symposium*, Vitória, Espírito Santo, Brazil, pp. 6 (in Portuguese).
- Rouse, J.W., Haas, R.H., Schell, J.A., Deering, D.W. & Harlan, J.C. 1973. Monitoring the vernal advancement of retrogradation of natural vegetation. *Greenbelt: National Aerospace Spatial administration*, 371 pp.
- Santana, L.S., Ferraz, G.A e S., Santos, S.A. Dos. & Dias, J.E.L. 2022. Precision coffee growing: A review. *Coffee Science* **17**, p. e172007.
- Santos, L.M., Ferraz, G.A.S., Andrade, M.T., Santana, L.S., Barbosa, B.D.S., Maciel, D.T. & Rossi, G. 2019a. Analysis of flight parameters and georeferencing of images with different control points obtained by RPA. *Agronomy Research* **17**(5), 2054–2063.
- Santos, P.L.F., Oliveira, R.M.M. & Gazola, R.P.D. 2019b. Photosynthetic pigments and their correlation with foliar nitrogen and magnesium in Bermuda grass grown in substrates. *Acta Iguacu* **8**, 92–101 (in Portuguese).
- Santos, L.M., Ferraz, G.A.S., Carvalho, M.A.F., Vilela, M.S. & Estima, P.H.O. 2023. Preliminary study on the potential use of RPA images to quantify the influence of the defoliation after coffee harvesting to its yield. *Agronomy Research* **21**(S3), 1555–1566.
- Santos, L.M., Ferraz, G.A.S., Carvalho, M.A. De F., Teodoro, S.A., Campos, A.A.V. & Menicucci Neto, P. 2022. Use of RPA Images in the Mapping of the Chlorophyll Index of Coffee Plants. *Sustainability* **14**, 13118.
- Shiratsuchi, L.S., Brandão, Z.N., Vicente, L.E., Victoria, D.D.C., Ducati, J.R., Oliveira, R.D. & Vilela, M.D.F. 2014. Remote Sensing: basic concepts and applications in Precision Agriculture. In: Bernardi, A.C. de C., Naime, J.M., Resende, A.V., Bassoi, L.H. & Inamasu, R. Y. (eds), Precision Agriculture (Results from a New Look). *Embrapa Instrumentação (ALICE)*, São Carlos- São Paulo, Brazil, 58–73 (in Portuguese).
- Vieira, S.R. 2000. Geostatistics in studies of spatial soil variability. In: Novais, R.F., Alvarez, V.V.H., Schaefer, C.E.G.R. (eds), *Special topics in soil sciences*. Brazilian Society of Soil Science, Viçosa, 1–54 (in Portuguese).
- Yu, K., Lenz-Wiedemann, V., Chen, X. & Bareth, G. 2014. Estimating leaf chlorophyll of barley at different growth stages using spectral indices to reduce soil background and canopy structure effects. *ISPRS* **97**, 58–77.
- Zanzarini, F.V., Pissarra, T.C., Brandão, F.J. & Teixeira, D.D. 2013. Spatial correlation of the vegetation index (NDVI) from Landsat /ETM+ images with soil attributes. *R. Bras. Agricultural Eng. Environmental* **17**(6), 608–614.